

TRANSVERSE-COHERENCE PROPERTIES OF THE FEL AT THE LCLS*

Yuantao Ding[†], Zhirong Huang, SLAC National Accelerator Laboratory, Menlo Park, CA, USA
 Samuel A. Ocko, Department of Physics, Massachusetts Institute of Technology, Cambridge, MA, USA

Abstract

The recently commissioned Linac Coherent Light Source is an x-ray free-electron laser at the SLAC National Accelerator Laboratory, which is now operating at x-ray wavelengths of 20-1.2 Angstrom with peak brightness nearly ten orders of magnitude beyond conventional synchrotron sources. Understanding of coherence properties of the radiation from SASE FELs at LCLS is of great practical importance for some user experiments. We present the numerical analysis of the coherence properties at different wavelengths based on a fast algorithm using ideal and start-end simulated FEL fields.

INTRODUCTION

The successful commissioning and operation of the linac coherent light source (LCLS) [1] has demonstrated that the x-ray free-electron laser (FEL) has come of age; these types of x-ray sources are poised to revolutionize the ultra-fast x-ray sciences. The LCLS and other hard x-ray FELs under construction are based on the principle of self-amplified spontaneous emission (SASE) [2, 3], where the amplification process starts from the shot noise in the electron beam. A large number of transverse radiation modes are also excited when the electron beam enters the undulator. The FEL collective instability in the electron beam causes the modulation of the electron density to increase exponentially, and after sufficient undulator distances, a single transverse mode starts to dominate. As a result, SASE FEL is almost fully coherent in the transverse dimension.

Understanding of transverse coherence properties of the radiation from SASE FELs is of great practical importance. The longitudinal coherence properties of SASE FELs have been studied before [4]. Some studies on the transverse coherence can be found in previous papers, for example, in ref. [5, 6, 7, 8, 9]. In this paper, we first discuss a new numerical algorithm based on Markov chain Monte Carlo techniques to calculate the FEL transverse coherence. Then we focus on the numerical analysis of the LCLS FEL transverse coherence.

BASIC DESCRIPTION OF TRANSVERSE COHERENCE

Many of the statistical properties of light can be described by the mutual coherence function [10],

$$\Gamma(\mathbf{r}_1, \mathbf{r}_2, \tau) = \langle E(\mathbf{r}_1, t) E^*(\mathbf{r}_2, t + \tau) \rangle, \quad (1)$$

where \mathbf{r}_1 and \mathbf{r}_2 are positions, and $E(\mathbf{r}, t)$ is the slowly varying amplitude of the amplified wave. The averaging symbol $\langle \dots \rangle$ means the ensemble average. In this study, we consider a stationary (ergodic) random process, which means an average calculated across the ensemble (i.e., an ensemble average) is equal to the same average calculated along a sample function (i.e., a time average). Thus we can calculate the coherence function with a time average along an x-ray pulse and it does not depend on t . We further assume the field $E(\mathbf{r}, t)$ is quasi-monochromatic, so the time delay due to the path length difference from \mathbf{r}_1 and \mathbf{r}_2 is negligible, and we don't have to include the temporal coherence effects. In this case, we can write the mutual coherence function to be mutual intensity function

$$J_{12} = J(\mathbf{r}_1, \mathbf{r}_2) = \Gamma(\mathbf{r}_1, \mathbf{r}_2, 0). \quad (2)$$

A further simplification is to introduce a normalization of the coherence function, hence we write the degree of transverse coherence:

$$\zeta = \frac{\int \int |J_{12}|^2 d\mathbf{r}_1 d\mathbf{r}_2}{\int J_{11} d\mathbf{r}_1 \int J_{22} d\mathbf{r}_2}. \quad (3)$$

Note that $\int J_{11} d\mathbf{r}_1 = \int J_{22} d\mathbf{r}_2 = P$, and P is the radiation power.

NUMERICAL METHOD

Based on the simulated radiation field (such as the dumped field from Genesis simulations), we could calculate the degree of transverse coherence through simply summing all terms in Eq.(3). However, the required computing power for such a brute force approach is huge, as we would need to integrate over all pairs of points $(\mathbf{r}_1, \mathbf{r}_2)$ in each longitudinal slice. For example, in a typical x-ray FEL simulation each longitudinal slice contains $100 \cdot 100$ cells in the transverse dimension and would require the calculation of 100 million different J_{12} . We could reduce this by a factor of two using the Hermitian property of the J matrix as $J_{12} = J_{21}^*$, but it's still a fairly unwieldy calculation.

We propose here to introduce Markov chain Monte Carlo techniques [11] to calculate the transverse coherence. We begin by rewriting the degree of transverse coherence as:

$$\zeta = \int d\mathbf{r}_1 d\mathbf{r}_2 \frac{|J_{12}|^2}{J_{11} J_{22}} \frac{J_{11} J_{22}}{P^2} = \int d\mathbf{r}_1 d\mathbf{r}_2 f(\mathbf{r}_1, \mathbf{r}_2) \mathcal{P}(\mathbf{r}_1, \mathbf{r}_2). \quad (4)$$

Where $f(\mathbf{r}_1, \mathbf{r}_2) = \frac{|J_{12}|^2}{J_{11} J_{22}}, \quad (5)$

and $\mathcal{P}(\mathbf{r}_1, \mathbf{r}_2) = \frac{J_{11} J_{22}}{P^2}. \quad (6)$

With this form, we can treat $\mathcal{P}(\mathbf{r}_1, \mathbf{r}_2)$ as a probability, as $\int \int \mathcal{P}(\mathbf{r}_1, \mathbf{r}_2) d\mathbf{r}_1 d\mathbf{r}_2 = 1$. Therefore, we can estimate ζ

* Work supported by the U.S. DOE contract nDE-AC02-76SF00515.

[†] ding@slac.stanford.edu

Table 1: Main Parameters for the LCLS FEL Simulations

Parameter	soft	hard	unit
electron beam energy	4.3	13.64	GeV
electron bunch charge	250	250	pC
rms energy spread	1.4	1.4	MeV
bunch peak current	1.5	3/1.5	kA
slice emittance	0.4	0.4	μm
average beta function	10	30	m
undulator period λ_u	3	3	cm
undulator parameter K	3.5	3.5	
FEL wavelength	1.5	0.15	nm
FEL ρ parameter	1	0.58/0.46	10^{-3}
saturation length [†]	~ 30	$\sim 80 - 90$	m

by sampling $f(\mathbf{r}_1, \mathbf{r}_2)$ with probability $\mathcal{P}(\mathbf{r}_1, \mathbf{r}_2)$. This can be done using a random weighted walk through the state space, where each state α represents a pair of transverse points $(\mathbf{r}_1, \mathbf{r}_2)$. In our implementation, the Metropolis-Hastings algorithm was used.

Markov chain Monte Carlo algorithms have the significant advantage over more naïve Monte Carlo algorithms in that most of the time is spent sampling from the most important terms in the summation. This makes a Markov chain Monte Carlo approach faster, as most states α have a very low probability since the beam is concentrated in the middle of each longitudinal slice.

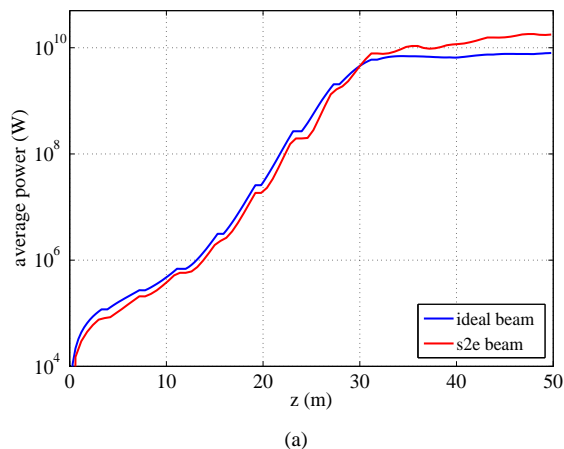
Initial states of the random walk are generated through rejection sampling, where we propose states with uniform probability and then only accept them with probability proportional to $\mathcal{P}(\alpha)$. This algorithm returns the correct distribution of α . In our implementation, $\mathcal{P}(\alpha) = \mathcal{P}(\mathbf{r}_1)\mathcal{P}(\mathbf{r}_2)$, so values of \mathbf{r}_1 and \mathbf{r}_2 can be generated independently from each other, speeding up the algorithm significantly.

Compared with the brute force algorithm, which simply sums over all terms in Eq. (3), the Markov chain Monte Carlo approach works about 100 times faster. For example, for a typical radiation field with $100 \cdot 100$ cells in transverse dimension, it converges within 45 seconds while obtaining a reasonable error bar. Sampling is done using several hundred independent random walks to get reliable error bars.

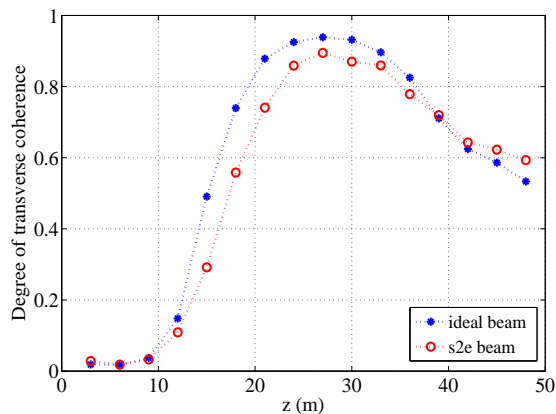
EVOLUTION OF TRANSVERSE COHERENCE IN LCLS FELS

We use 3D FEL code Genesis 1.3 [12] to simulate the SASE radiation produced by the LCLS undulator and use the Monte Carlo techniques described in the previous section to analyze the degree of transverse coherence. The main parameters are listed in Table 1. For both soft and hard x-rays, we performed the FEL simulations using ideal electron beam and start-to-end (S2E) simulated electron beam respectively.

[†]This is the total undulator beam line length including the breaks between undulator sections.



(a)



(b)

Figure 1: FEL power evolution (a) and degree of transverse coherence (b) along the undulator distance for soft x-rays at 1.5 nm wavelength based on an ideal electron beam (blue curves) and S2E beam (red curves). Note the undulator distance includes the breaks between undulator sections in all the figures in this paper.

Soft x-ray FELs

We first analyze the transverse coherence properties for the LCLS soft x-ray FELs at 1.5 nm wavelength. The main parameters used for an ideal beam are listed in Table 1, where we choose the peak current of 1.5 kA. The slice beam parameters from S2E simulations are very similar with those listed in Table 1 for the core part, but with double horns on the current profile due to wakefields in the linac structures. Figure 1(a) and 1(b) show the FEL power evolution and the degree of transverse coherence along the undulator. The FEL power saturates at about $z = 30$ m for both ideal beam and S2E beam. The transverse coherence develops quickly in the exponential gain regime and reaches maximum of about 90 – 95% at about $z = 27$ m, a few meters before the FEL power saturation. The difference between the ideal beam and S2E beam is small in this setup.

Hard x-ray FELs

We choose the wavelength of 1.5 \AA for hard x-ray analysis, which is the typical hard x-ray radiation wavelength at LCLS. At this wavelength, the typical operating current is 3 kA. We first study the coherence using 3 kA for an ideal beam and S2E beam (core part), and will also discuss the case with 1.5 kA current.

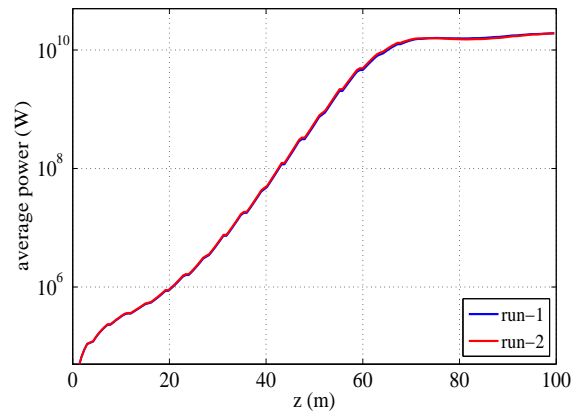
For an ideal beam at 3 kA, the FEL power saturates at about $z = 70\text{m}$ (Fig. 2(a)), and the degree of transverse coherence peaks at about $z = 60\text{m}$ with a maximum of 0.85-0.9 (Fig. 2(b)). In this study we changed the initial seed for shot noise in FEL simulations, and we can see that the results are very similar on the degree of transverse coherence with different shot noise seeds.

For a S2E beam at 3 kA, as shown in Fig. 3(a) and Fig. 3(b), the FEL power saturates at about $z = 80\text{m}$, and the degree of transverse coherence peaks at about $z = 78\text{m}$ with a maximum value of 0.65. Compared with the ideal beam, the maximum coherence dropped from 0.85 to 0.65. The double-horn current profile and non-uniformity of the slice beam properties may cause this degradation of the transverse coherence. For the beam current of 3 kA with double horns, the slice emittance and energy spread are much larger at the bunch tails, and the resistive wall wakefields also introduce additional energy variation along the bunch. Due to these effects, the FEL gain varies at different slices of the bunch. As we already see from Fig. 2(b), for an ideal beam, the transverse coherence peaks just before FEL saturation, then drops after saturation. Now with the S2E beam, we can never make the different slices saturate at the same time. So when we do a time average to calculate the transverse coherence over the different slices, the transverse coherence degrades.

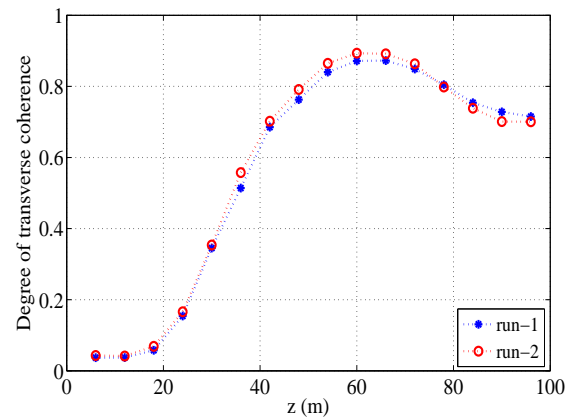
One possible way to improve the transverse coherence for a real beam, such as LCLS hard x-rays, is to reduce the peak current, as double-horn and non-uniformity effects will be reduced. At LCLS we have enough undulator sections to get FEL saturation with a lower peak current. In S2E simulations, by tuning the L2 rf phase about 2 degrees to get less compression in the second bunch compressor, we obtained a peak current of 1.5 kA on the core part of the beam. The FEL power gain curve and degree of transverse coherence along the undulator at this peak current are shown in Fig. 4. We see that the degree of transverse coherence increased to a maximum of above 0.8 with 1.5kA. At the same time, the divergence of the FEL light for this case is reduced by about 20% compared with 3 kA case.

CONCLUSIONS

We developed a new algorithm based on Markov chain Monte Carlo techniques to analyze the FEL transverse coherence from simulated FEL fields. For a SASE FEL such as LCLS, we observed high degree (about 90%) of transverse coherence using an ideal beam at close to FEL saturation point. From a S2E beam, the degree of transverse coherence is reduced due to the non-uniformity of the slice



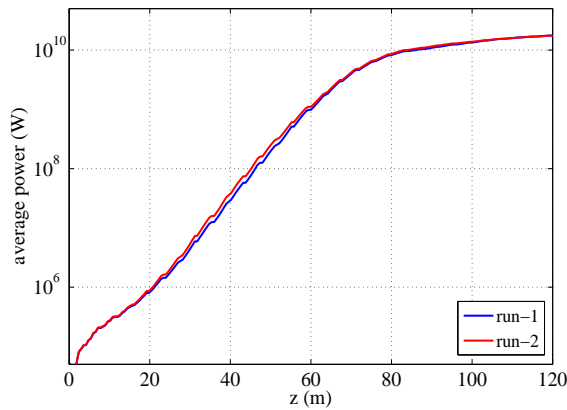
(a)



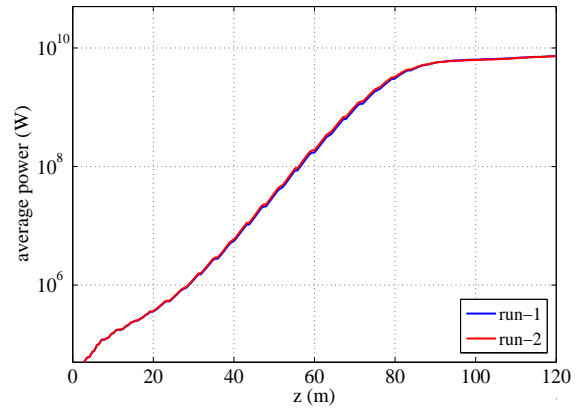
(b)

Figure 2: FEL power evolution (a) and degree of transverse coherence (b) along the undulator distance for hard x-rays at 1.5 \AA wavelength based on an ideal electron beam (3 kA). Two curves show the results using different initial seed for shot noise.

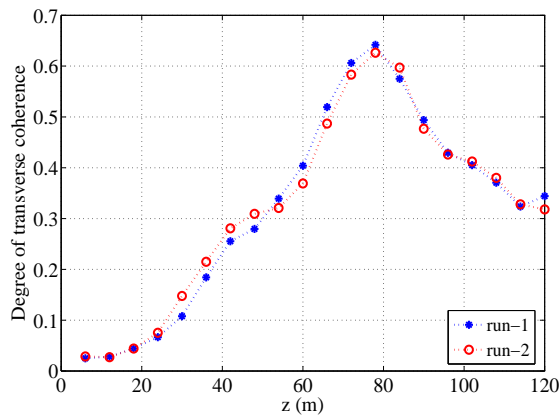
beam parameters. For soft x-ray, since we typically operate at 1.5 kA, we still observe a very highly coherent beam. But for hard x-ray, if we operate at 3 kA, the degree of transverse coherence could be reduced to about 65%. However, this can be improved by operating the machine at a peak current of 1.5 kA, where the degree of the transverse coherence reaches over 80% at the peak. With less compression, the collective effects are weaker, and the saturation length is only about 10 m longer than the case with 3 kA, but the x-ray pulse length is doubled. Also note that the transverse coherence degrades after saturation. Tapering undulator after saturation may increase the total FEL output energy by a factor of 2, but get lower degree of transverse coherence.



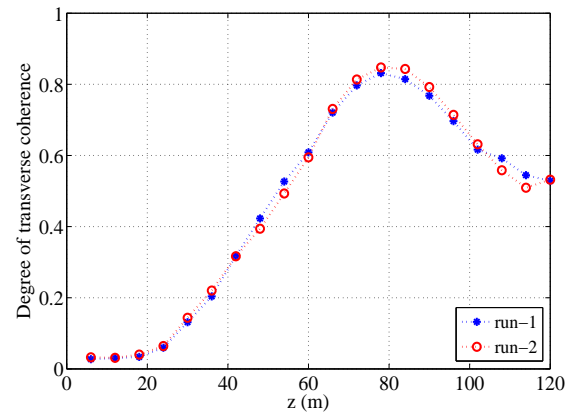
(a)



(a)



(b)



(b)

Figure 3: FEL power evolution (a) and degree of transverse coherence (b) along the undulator distance for hard x-ray at 1.5 Å wavelength based on a S2E electron beam (3kA). Two curves show the results using different initial seed for shot noise.

Figure 4: FEL power evolution (a) and degree of transverse coherence (b) along the undulator distance for hard x-ray at 1.5 Å wavelength based on a S2E electron beam (1.5kA). Two curves show the results using different initial seed for shot noise.

REFERENCES

- [1] P. Emma et al, Nature Photonics, Published online: 1 August 2010 — doi:10.1038/nphoton.2010.176.
- [2] K. Kondratenko and E. Saldin, Part. Accel. 10, 207216 (1980);
- [3] R. Bonifacio, R., C. Pellegrini, L. M. Narducci, Opt. Commun. 50, 373378 (1984).
- [4] see, for example, E.L. Saldin, E.A. Schneidmiller, M.V. Yurkov, Opt. Commun. **148**, 383 (1998).
- [5] E.L. Saldin, E.A. Schneidmiller, M.V. Yurkov, Opt. Commun. **186**, 185 (2000).
- [6] V. Kumar, S. Krishnagopal, Nucl. Instrum. Meth. A **445**,73 (2000).
- [7] E.L. Saldin, E.A. Schneidmiller, M.V. Yurkov, Nucl. Instrum. Meth. A **507**, 106 (2003).
- [8] S. Reiche, PAC 07 proceedings (Albuquerque, New Mexico), P1272.
- [9] E.L. Saldin, E.A. Schneidmiller, M.V. Yurkov, Opt. Commun. **281**, 1179 (2008).
- [10] see, for example, J. W. Goodman, "Statistical Optics", Wiley, 1985.
- [11] see http://en.wikipedia.org/wiki/Markov_chain_Monte_Carlo.
- [12] S. Reiche, Nucl. Instrum. Meth. A **429**, 243 (1999).